

Figure 1. A and B forms of bianthrone (1).

it to determine otherwise inaccessible standard potentials, standard heterogeneous electron-transfer rate constants, and rate constants of following chemical reactions. As applied to the reduction of bianthrone, homogeneous redox catalysis should permit an independent determination of  $k_{AB^-}$  and  $E_{1A}^\circ$ , quantities that are very difficult to measure but whose determination is essential to a complete understanding of the redox reactions of this class of substances.

### Experimental Section

Dimethylformamide (DMF, Burdick and Jackson) was vacuum distilled and stored over Woelm 200 neutral alumina (activated at 300 °C under nitrogen for 24 h). The supporting electrolyte was 0.10 M tetraethylammonium perchlorate.<sup>2a</sup> Bianthrone and 1,1'-dimethylbianthrone were obtained from Aldrich Chemical Co. and used as received. All solutions were protected from exposure to atmospheric moisture, and solutions containing either of the bianthrones were kept in the dark.

Voltammetry was performed with a Princeton Applied Research Model 170 electrochemistry system and a cell of the type previously reported.<sup>5</sup> The working electrode was a hanging mercury drop,<sup>6</sup> whose area was about 0.016 cm<sup>2</sup>. The silver reference electrode (AgRE) was a silver wire in contact with 0.010 M AgNO<sub>3</sub>, 0.10 M tetraethylammonium perchlorate in DMF,<sup>7</sup> whose potential was found to be +0.423 V vs. aqueous SCE. Solutions were purged with purified nitrogen and were maintained at 25.0 °C.

The catalytic effects measured in this work were relatively modest. In order to observe a measurable catalytic current, it was necessary to employ slow scan rates, which required a modification of the procedures used for data analysis. The available theoretical results<sup>4c</sup> pertain to linear diffusion and will not be expected to describe rigorously the present experiments that used spherical electrodes and slow scan rates. Therefore, theoretical working curves pertaining to spherical diffusion were generated by digital simulation. The simulation technique was normal<sup>8</sup> with the exception of the treatment of the chemical reactions (reactions 2, 3, and 5) that were combined to give finite difference representations of  $dC_i/dt$  for the six species in the scheme with the assumptions that A<sup>-</sup> and B<sup>-</sup> were at steady state and reaction 5 was a fast equilibrium. The simulations agreed well with the results for linear diffusion<sup>4c</sup> when the spherical parameter  $\phi$  was set equal to zero ( $\phi = (DRT/Fv)^{1/2}$  where  $D$  is the diffusion coefficient of the catalyst,  $v$  is the sweep rate, and  $r$  is the electrode radius). Use of the spherical working curves resulted in slightly different values of the rate constants than would have been obtained with the linear-diffusion working curves. The maximum difference is about 25%.

The catalysis observed with the three quinone catalysts with the least negative formal potentials was so weak that another change in procedure was instituted. Normally, the peak current for quinone reduction was measured in the presence ( $i_p$ ) and the absence ( $i_d$ ) of bianthrone. For weak catalysis,  $i_p/i_d$  was close to unity and errors from two separate experiments combined to impart considerable uncertainty to the ratio. A way was sought to measure the catalytic effect from a single experiment. This was achieved by measurement of the ratio of the anodic peak current (for oxidation of quinone radical anion) to the cathodic peak current (for reduction of quinone). This ratio will be unity when no catalysis occurs and will decrease slightly for weak catalysis. Working curves were generated by use of the digital simulation technique discussed above.

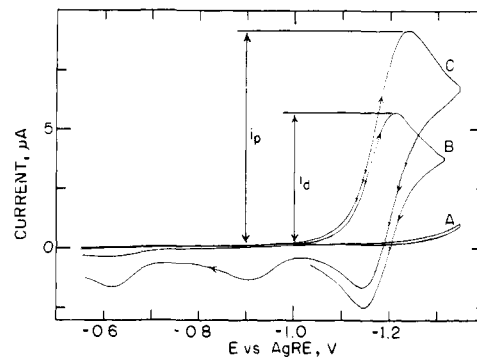
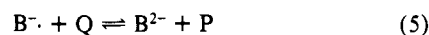
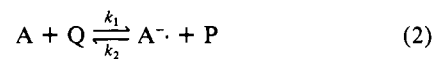


Figure 2. Cyclic voltammograms in 0.10 M tetraethylammonium perchlorate/DMF: (A) 1.00 mM bianthrone (1); (B) 2.00 mM duroquinone; (C) 1.00 mM 1 + 2.00 mM duroquinone. Sweep rate: 0.050 V s<sup>-1</sup>.

### Results

Figure 2 shows cyclic voltammograms of the catalyst duroquinone in the absence and presence of bianthrone. The catalytic effect manifests itself through an increased reduction peak current  $i_p$  when bianthrone is present compared to the diffusion-controlled peak current  $i_d$  obtained with no bianthrone.

The catalysis is postulated to occur by the following reaction scheme:<sup>9</sup>



where P is the quinone and Q its radical anion. The occurrence of reactions 2 and 5 results in regeneration of P near the electrode to give the observed increase in current. The equilibrium state of reaction 2 favors the reactants, but the occurrence of the rapid and essentially irreversible reaction 3 can cause reaction 2 to proceed to an appreciable extent in the forward direction. For the quinone catalysts studied in this work, the equilibrium state of reaction 5 lies almost completely to the right and the reaction will be considered to be very fast.

Qualitative evidence for the occurrence of the homogeneous redox-catalyzed reduction of bianthrone via reactions 1–5 was provided<sup>2d</sup> by the observed increase in the peak for P reduction (as in curve C, Figure 2), a decrease in the peak height for Q oxidation, a decrease in the peak height for the direct reduction of bianthrone ( $E_p = -1.43$  V), and the appearance on the positive-going scan of peaks for the stepwise oxidation of the product of the catalytic reduction, B<sup>2-</sup> (oxidation peaks at -0.9 and -0.6 V, curve C, Figure 2).

A quantitative characterization of the catalysis requires measurement<sup>4c</sup> of  $i_p/i_d$  at various scan rates, catalyst concentrations, and ratios of bianthrone concentration to catalyst concentration,  $\gamma$ . Two kinetic regimes exist.<sup>4c</sup> When the reaction rate is controlled by forward reaction 2,  $i_p/i_d$  will increase as  $C_P^*$  is increased at constant  $\gamma$ . When the rate is controlled by reaction 3 with 2 as a preequilibrium,  $i_p/i_d$  is independent of  $C_P^*$  if  $\gamma$  is held constant. Some systems will fall in the region of mixed control by both reactions 2 and 3.

Redox catalysis by duroquinone corresponds to rate control by forward reaction 2 under most conditions with transition to mixed control at high catalyst concentrations. The data in Table I have been analyzed with the aid of theoretical working curves for control by forward reaction 2 (see Experimental Section) and satisfactorily

(5) Buchta, R. C.; Evans, D. H. *Anal. Chem.* **1968**, *40*, 2181–6.

(6) Whitson, P. E.; VandenBorn, H. W.; Evans, D. H. *Anal. Chem.* **1973**, *45*, 1298–1306.

(7) Ryan, M. D.; Evans, D. H. *J. Electroanal. Chem. Interfacial Electrochem.* **1976**, *67*, 333–57.

(8) Feldberg, S. W. In "Electroanalytical Chemistry"; Bard, A. J., Ed.; Marcel Dekker: New York, 1969; pp 199–296.

(9) Symbols and definitions are patterned after ref 4a–e.

Table I. Redox-Catalyzed Reduction of Bianthrone with Duroquinone as Catalyst ( $E^{\circ}_{PQ} = -1.17_7$  V)<sup>a</sup>

$C_P^*$ , mM	$\nu$ , V s <sup>-1</sup>	$\gamma = 2.0$		$\gamma = 1.0$		$\gamma = 0.50$	
		$i_p/i_d$	$\log k_1$ , L mol <sup>-1</sup> s <sup>-1</sup>	$i_p/i_d$	$\log k_1$ , L mol <sup>-1</sup> s <sup>-1</sup>	$i_p/i_d$	$\log k_1$ , L mol <sup>-1</sup> s <sup>-1</sup>
0.5	0.20	1.36	3.07	1.16	3.05		
	0.10	1.70	3.11	1.37	3.14		
	0.05	2.12	3.11	1.55	3.07		
1.0	0.20	1.69	3.10	1.34	3.08	1.15	3.06
	0.10	2.08	3.08	1.60	3.09	1.27	3.04
	0.05	2.50	3.02	1.89	3.07	1.43	3.02
2.0	0.20	1.89	2.94	1.41	2.86	1.20	2.88
	0.10	2.32	2.91	1.73	2.92	1.34	2.86
	0.05	2.92	2.92	1.98	2.86	1.56	2.85
4.0	0.20					1.28	2.77
	0.10					1.45	2.74
	0.05					1.64	2.72

<sup>a</sup> Analysis assumes rate control by forward reaction 2.  $C_P^*$  = catalyst concentration,  $\nu$  = scan rate,  $\gamma$  = excess factor (ratio of bianthrone concentration to catalyst concentration),  $i_p$  = observed peak or plateau current,  $i_d$  = catalyst peak current in the absence of bianthrone,  $k_1$  = forward rate constant for reaction 2.  $C_P^* = 0.5$  mM,  $\gamma = 0.50$  gives negligible catalysis.  $C_P^* = 4.0$  mM,  $\gamma = 2.0$  and 1.0 could not be studied due to limited solubility of bianthrone.  $E^{\circ}_{PQ}$  taken as midpoint between peak potentials of quinone couple (vs. AgRE).

Table II. Redox-Catalyzed Reduction of Bianthrone with Duroquinone as Catalyst ( $E^{\circ}_{PQ} = -1.17_7$  V)<sup>a</sup>

$C_P^*$ , mM	$\nu$ , V s <sup>-1</sup>	$\gamma = 2.0$		$\gamma = 1.0$		$\gamma = 0.50$	
		$i_p/i_d$	$\log(k_{AB^-}/k_2)$ , mol L <sup>-1</sup>	$i_p/i_d$	$\log(k_{AB^-}/k_2)$ , mol L <sup>-1</sup>	$i_p/i_d$	$\log(k_{AB^-}/k_2)$ , mol L <sup>-1</sup>
2.0	0.20	1.89	-2.80	1.41	-2.95	1.20	-2.90
	0.10	2.32	-2.95	1.73	-2.94	1.34	-2.98
	0.05	2.92	-2.97	1.98	-3.10	1.53	-3.05
4.0	0.20					1.28	-2.87
	0.10					1.45	-2.97
	0.05					1.64	-3.03

<sup>a</sup> Analysis assumes mixed control by reactions 2 and 3.

Table III. Redox-Catalyzed Reduction of Bianthrone with 2-Chloro-9,10-anthraquinone as Catalyst ( $E^{\circ}_{PQ} = -1.16_3$  V)<sup>a</sup>

$C_P^*$ , mM	$\nu$ , V s <sup>-1</sup>	$\gamma = 2.0$		$\gamma = 1.0$		$\gamma = 0.50$	
		$i_p/i_d$	$\log k_1$ , L mol <sup>-1</sup> s <sup>-1</sup>	$i_p/i_d$	$\log k_1$ , L mol <sup>-1</sup> s <sup>-1</sup>	$i_p/i_d$	$\log k_1$ , L mol <sup>-1</sup> s <sup>-1</sup>
0.5	0.20	1.18	2.76	1.08	2.79		
	0.10	1.35	2.78	1.14	2.69		
	0.05	1.63	2.76	1.31	2.74		
1.0	0.20	1.28	2.69	1.14	2.69	1.07	2.71
	0.10	1.64	2.77	1.28	2.72	1.14	2.74
	0.05	1.99	2.74	1.54	2.75	1.26	2.74
2.0	0.20			1.17	-3.00		
	0.10			1.37	-2.95	1.15	-3.05
	0.05			1.65	-2.95	1.32	-3.00
4.0	0.20			1.22	-3.05	1.14	-2.85
	0.10			1.47	-3.05	1.28	-2.85
	0.05			1.74	-3.06	1.45	-2.90
8.0	0.20					1.17	-2.93
	0.10					1.33	-2.90

<sup>a</sup> Analysis of  $C_P^* = 0.5$  and 1.0 mM data assumes rate control by forward reaction 2. Analysis of remaining data assumes mixed control.

constant values of  $k_1$  were obtained for catalyst concentrations of 0.5 and 1.0 mM. The mean value was  $\log k_1 = 3.07 \pm 0.03$ . However, there is a significant reduction in  $k_1$  obtained at  $C_P^* = 2.0$  and 4.0 mM due to transition to the mixed control region.

Mixed control theoretical working curves were constructed for each value of  $\gamma$ . Separate plots of  $i_p/i_d$  vs.  $\log k_{AB^-}/k_2 C_P^*$  were prepared for each value of  $\log(k_1 C_P^*/a)$  where  $a = Fv/RT$ . The required values of  $\log(k_1 C_P^*/a)$  were calculated on the basis of  $\log k_1 = 3.07$  as evaluated above, and the results for 2.0 and 4.0 mM duroquinone are summarized in Table II. The fact that the catalysis is partially controlled by the  $A^- \rightarrow B^-$  reaction permits evaluation of  $k_{AB^-}/k_2$  from the data. The mean value obtained was  $\log(k_{AB^-}/k_2) = -2.96 \pm 0.08$ .

Table IV. Summary of Bianthrone Rate Constants

catalyst	$E^{\circ}_{PQ}$ , V vs. AgRE	$\log k_1$ , L mol <sup>-1</sup> s <sup>-1</sup>	$\log k_{AB^-}/k_2$ , mol L <sup>-1</sup>
duroquinone	-1.17 <sub>7</sub>	3.07 ± 0.03	-2.96 ± 0.08
2-chloro-9,10-anthraquinone	-1.16 <sub>3</sub>	2.74 ± 0.03	-2.96 ± 0.08
2-methyl-1,4-naphthoquinone	-1.11 <sub>0</sub>	1.88 ± 0.03	
2,6-dimethoxy-1,4-benzoquinone	-1.08 <sub>8</sub>	1.50 ± 0.06	
2,5-di- <i>tert</i> -butyl-1,4-benzoquinone	-1.05 <sub>0</sub>	1.10 ± 0.07	

**Table V.** Redox-Catalyzed Reduction of Bianthrone with Duroquinone as Catalyst in 90:10 DMF/CH<sub>3</sub>OH ( $E^{\circ}_{PQ} = -1.13_4$  V)<sup>a</sup>

$C_P^*$ , mM	$\nu$ , V s <sup>-1</sup>	$i_p/i_d$	$\log k_1$ , L mol <sup>-1</sup> s <sup>-1</sup>
0.5	0.10	1.09	2.52
	0.05	1.20	2.56
1.0	0.10	1.12	2.32
	0.05	1.21	2.29
2.0	0.10	1.25	2.37
	0.05	1.37	2.21

<sup>a</sup> Analysis assumes rate control by forward reaction 2.  $\gamma = 1.0$ .

**Table VI.** Redox-Catalyzed Reduction of 1,1'-Dimethylbianthrone with 1,4-Diamino-5-nitro-9,10-anthraquinone as Catalyst ( $E^{\circ}_{PQ} = -1.37_6$  V)<sup>a</sup>

$C_P^*$ , mM	$\nu$ , V s <sup>-1</sup>	$i_p/i_d$	$\log(k_{AB^-} k_1/k_2)$ , s <sup>-1</sup>
1.0	0.20	1.29	-0.60
	0.10	1.52	-0.66
	0.05	1.87	-0.64
2.0	0.20	1.24	-0.64
	0.10	1.51	-0.67
	0.05	1.81	-0.70
4.0	0.20	1.27	-0.62
	0.10	1.56	-0.62
	0.05	1.86	-0.65
			-0.64 ± 0.03

<sup>a</sup> Analysis assumes rate control by reaction 3.  $\gamma = 1.0$ .

Results were then obtained for a catalyst with a slightly more positive standard potential, 2-chloro-9,10-anthraquinone ( $E^{\circ}_{PQ} = -1.16_3$  V), and analogous behavior was observed. The catalysis was under control of forward reaction 2 for  $C_P^* = 0.5$  and 1.0 mM and under mixed control for  $C_P^* = 2.0, 4.0,$  and 8.0 mM. The results are summarized in Table III, and mean values of the rate constants are listed in Table IV.

Catalysis by quinone couples with still more positive potentials was exceedingly weak. The low solubility of bianthrone prevented the use of high values of  $\gamma$  where catalysis would be more pronounced. Three additional quinones were studied ( $C_P^* = 1.0$  mM,  $\gamma = 1.0$ ), and the data were analyzed by evaluation of the decrease in the anodic peak for  $Q \rightarrow P + e$  because the values of  $i_p/i_d$  were too close to unity for accurate determination of  $k_1$  in the manner employed earlier. The average values of  $k_1$  are included in Table IV.

Catalysis of bianthrone reduction by duroquinone was also studied in 90:10 DMF/CH<sub>3</sub>OH (by volume), and the results are summarized in Table V. The overall rate of catalysis is somewhat smaller, as may be seen from a comparison of the values of  $i_p/i_d$  in Table V with those in Table I obtained under corresponding conditions. The data have been treated on the assumption that the rate is controlled by forward reaction 2. The values of  $k_1$  so obtained decrease as  $C_P^*$  increases, signifying transition to the region of mixed control. The value of  $\log k_1 = 2.54$  obtained at the lowest catalyst concentration is considered to be the most reliable.

The rate of the  $A^- \rightarrow B^-$  reaction is known to be much slower for 1,1'-dimethylbianthrone (**2**) than for bianthrone itself.<sup>2b</sup> In **2** (*E* isomer), one methyl group is attached to each ring system at the position closest to the double bond connecting the two systems. The smaller value of  $k_{AB^-}$  is attributed to steric hindrance in the necessary passage of a methyl group past a hydrogen atom on the opposite ring system during the  $A^- \rightarrow B^-$  reaction.

Results for the redox-catalyzed reduction of **2** by 1,4-diamino-5-nitro-9,10-anthraquinone are presented in Table VI. In this case,  $i_p/i_d$  is independent of  $C_P^*$ , signifying rate control by the  $A^- \rightarrow B^-$  reaction.<sup>4e</sup>

The peak potentials for the direct reduction of **1** and **2** can also provide information about  $E^{\circ}_{1A}$  and  $k_{AB^-}$ . If the electron-transfer

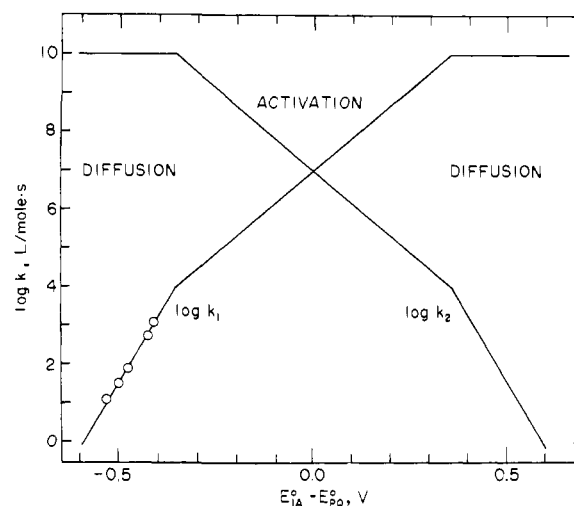


**Figure 3.** Rate constants for cross-electron-exchange reaction as functions of the difference between substrate and catalyst formal potentials. Data taken from Table IV and plotted by using  $E^{\circ}_{1A} = -1.589$  V.

reaction is quite fast, a range of sweep rates will exist in which the electrode reaction is governed by the rate of the  $A^- \rightarrow B^-$  reaction. Then the peak potential for this ECE scheme will be given by<sup>10</sup>

$$E_p = E^{\circ}_{1A} - 0.067 + (RT/2F) \ln k_{AB^-} - (RT/2F) \ln \nu \quad (6)$$

(For the cases where eq 6 will be used, the ECE mechanism as opposed to DISP1 is followed.<sup>10b</sup>) Thus  $E_p$  should shift 29.6 mV for each decade change in scan rate, and  $E_p$  at  $\nu = 1.00$  V/s will be  $E^{\circ}_{1A} - 0.067 + 0.0296 \log k_{AB^-}$ . The values of the experimental slopes and intercepts were for bianthrone in DMF (32 mV, -1.472 V); for bianthrone in 90:10 DMF/CH<sub>3</sub>OH (32 mV, -1.475 V); for 1,1'-dimethylbianthrone in DMF (40 mV, -1.654 V vs. AgRE).

## Discussion

The redox-catalyzed reduction of bianthrone in DMF is under the control of forward reaction 2, and values of  $k_1$  have been obtained for five catalyst couples whose formal potentials cover a range of 0.12 V. Reaction 2 is a cross electron exchange between the  $A/A^-$  and  $P/Q$  couples. For the series of quinones studied, the diffusion coefficients will be approximately equal as will the contribution of the catalyst couple to the free energy of activation. Under these conditions, the variations of  $k_1$  and  $k_2$  from one catalyst to another are functions of the difference between the formal potentials of the  $A/A^-$  and  $P/Q$  couples<sup>4f</sup> as shown in Figure 3.

The interpretation of Figure 3 will be aided by a consideration of the fundamental relationships between the rate constants ( $k_1$  and  $k_2$ ), the equilibrium constant of reaction 2, and the formal potentials as given by eq 7.

$$k_1/k_2 = K_2 = \exp((F/RT)(E^{\circ}_{1A} - E^{\circ}_{PQ})) \quad (7)$$

$$\log k_1 = \log k_2 + (1/0.0592)(E^{\circ}_{1A} - E^{\circ}_{PQ}) \quad (8)$$

Homogeneous redox catalysis can be studied when  $k_2 < 1$  (left half of Figure 2). When  $E^{\circ}_{PQ}$  is well removed from  $E^{\circ}_{1A}$ , the back reaction will occur at the diffusion-controlled rate (assumed<sup>4b</sup> to be  $10^{10}$  L mol<sup>-1</sup> s<sup>-1</sup>) for each quinone. From eq 8 it can be seen that the slope of a plot of  $\log k_1$  vs.  $(E^{\circ}_{1A} - E^{\circ}_{PQ})$  will be 1/59.2 mV<sup>-1</sup>. As  $E^{\circ}_{PQ}$  becomes closer to  $E^{\circ}_{1A}$ , a region of activation control is entered<sup>4f</sup> where the slope is lower (shown as 1/118 mV<sup>-1</sup> in Figure 3).

The experimental data plotted in Figure 3 give a slope of 1/60 mV<sup>-1</sup>, clearly showing that the system falls in the diffusion-con-

(10) (a) Mastragostino, M.; Nadjó, L.; Savéant, J. M. *Electrochim. Acta* 1968, 13, 721-49. (b) Amatore, C.; Savéant, J. M. *J. Electroanal. Chem. Interfacial Electrochem.* 1977, 85, 27-46.

trolled region. Values of  $k_1$  and  $E^{\circ}_{PQ}$  for each quinone were placed in eq 8, and an average value of  $E^{\circ}_{1A} = -1.589 \pm 0.004$  V was obtained.

This value of  $E^{\circ}_{1A}$  may be combined with the peak-potential data for the direct reduction of bianthrone to obtain  $k_{AB}^-$ . The value of  $E_p$  at  $v = 1$  V  $s^{-1}$  was  $-1.472$  V, which should equal  $E^{\circ}_{1A} - 0.067 + 0.0296 \log k_{AB}^-$  (cf. eq 6). The result is  $k_{AB}^- = 2 \times 10^6$   $s^{-1}$ , which is considerably larger than the value obtained in alkaline 2-propanol/water/THF by means of pulse radiolysis,<sup>2b</sup>  $7 \times 10^4$   $s^{-1}$ .

Studies in the mixed control region gave  $\log(k_{AB}/k_2) = -2.96$  (Table IV). Insertion of  $k_{AB}^- = 2 \times 10^6$   $s^{-1}$  gives  $k_2 = 2 \times 10^9$  L  $mol^{-1}$   $s^{-1}$ , which is of the expected order of magnitude for a diffusion-controlled reaction in DMF. This calculation supports the internal consistency of the analysis.

The fact that  $k_{AB}^-$  determined in this work in DMF is greater than the value determined earlier in alkaline 2-propanol/water/THF prompted us to explore the effect of solvent on  $k_{AB}^-$ . The most obvious difference is that DMF is not a hydrogen-bond donating solvent. Unfortunately, electrochemical experiments in 2-propanol/water/THF were not successful due to the low solubility of bianthrone and apparent instability of the quinone anion radicals as evidenced by oxidation peaks of less than theoretical height. However, it was possible to investigate redox catalysis in 90:10 DMF/CH<sub>3</sub>OH with duroquinone as catalyst, and the overall catalytic rate was lower (Table V). The value of  $\log k_1$  evaluated from the data obtained at the lowest catalyst concentration gives  $E^{\circ}_{1A} = -1.576$  V when calculated via eq 8. Again, this  $E^{\circ}_{1A}$  can be combined with the peak-potential data to give  $k_{AB}^- = 1 \times 10^6$   $s^{-1}$ , which is slightly smaller than in DMF alone but still 15 times greater than the pulse radiolysis value. Thus solvent composition appears to affect  $k_{AB}^-$ , but it is not known whether the remaining discrepancy between the result in 90:10 DMF/CH<sub>3</sub>OH and 69:20:10:1 2-propanol/water/THF/acetone<sup>2b</sup> is entirely a solvent effect.

The experimental value of  $E^{\circ}_{PQ}$  for duroquinone in 90:10 DMF/CH<sub>3</sub>OH was  $-1.134$  V, a 43-mV positive shift from the value in DMF alone, and the calculated value of  $E^{\circ}_{1A}$  showed a 13-mV positive shift. Positive shifts of this nature have been observed for other neutral/anion couples upon addition of a hydroxylic solvent to a dipolar aprotic solvent<sup>11</sup> and are normally attributed to stabilization of the anion through hydrogen bonding.

The rate of the  $A^- \rightarrow B^-$  reaction is known<sup>2b</sup> to be slower for 1,1'-dimethylbianthrone (**2**) than for bianthrone, and this qualitative conclusion was confirmed by the redox-catalysis studies, which showed that the system was in the region of rate control by reaction 3 with reaction 2 as a preequilibrium (Table VI). From the data we obtain  $\log(k_{AB}^-k_1/k_2) = -0.64$ .

One approach for calculating  $k_{AB}^-$  and  $E^{\circ}_{1A}$  is to insert the above result into eq 8 along with the measured value of  $E^{\circ}_{PQ}$  to produce eq 9, relating  $E^{\circ}_{1A}$  and  $k_{AB}^-$ . A second independent

$$0.0592 \log k_{AB}^- = -1.414 - E^{\circ}_{1A} \quad (9)$$

equation relating these two quantities is embodied in the peak potential for direct reduction of **2** at  $v = 1$  V  $s^{-1}$ , which equals  $E^{\circ}_{1A} - 0.067 + 0.0296 \log k_{AB}^-$ . Simultaneous solution of the two equations would give  $k_{AB}^-$  and  $E^{\circ}_{1A}$ .

Unfortunately, the peak-potential data are not entirely consistent with rate control by the  $A^- \rightarrow B^-$  reaction and  $A + e \rightleftharpoons A^-$  being very fast. In particular,  $dE_p/d(\log v)$  was found to be 40 mV, compared to a theoretical value<sup>10</sup> of 29.6 mV. Therefore, the peak-potential data will not be used.

However, it is possible to estimate a value for  $E^{\circ}_{1A}$  of  $-1.69 \pm 0.02$  V that is consistent with the experimental observations. The peak-potential data for direct reduction of **2** suggest partial rate control by the electron-transfer reaction, which means that the value of  $E_p$  at 1 V  $s^{-1}$  ( $-1.65$  V) is more negative than it would be if electron transfer were highly facile. The observed  $dE_p/d(\log$

$v)$  value and the value of  $k_{AB}^-$  obtained below were compared with theoretical data,<sup>12,13</sup> and  $E^{\circ}_{1A} = -1.70$  V was obtained. Also, at low temperatures it is possible to determine  $E^{\circ}_{1A}$  directly by cyclic voltammetry because the  $A^- \rightarrow B^-$  reaction is sufficiently slow to permit detection of an oxidation peak for  $A^-$ . The value obtained<sup>2g</sup> at  $-56$  °C in butyronitrile solvent is  $-1.68$  V vs. AgRE in butyronitrile.

Use of  $E^{\circ}_{1A} = -1.69 \pm 0.02$  V in eq 9 gives  $\log k_{AB}^- = 4.7 \pm 0.3$  or  $k_{AB}^- = 5 \times 10^4$   $s^{-1}$  for 1,1'-dimethylbianthrone in DMF at 25 °C. By contrast, the value found by pulse radiolysis in alkaline 2-propanol/water/THF was  $1.1 \times 10^3$   $s^{-1}$  at 21 °C.

Thus, the redox catalysis studies indicate that the values of  $k_{AB}^-$  in DMF for both bianthrone and 1,1'-dimethylbianthrone are considerably larger than those found by pulse radiolysis in a different solvent. Further support of the conclusion may be found by consideration of the results of cyclic voltammetry studies of the direct reduction of 1,1'-dimethylbianthrone. Of course, if  $k_{AB}^- = 5 \times 10^4$   $s^{-1}$ , it would be very difficult to detect  $A^-$  by cyclic voltammetry. It is necessary for  $k_{AB}^-RT/Fv$  to be less than about one in order to begin to discern an  $A^-$  oxidation peak in an ECE mechanism.<sup>14</sup> This would require  $v = 1300$  V  $s^{-1}$  if  $k_{AB}^- = 5 \times 10^4$   $s^{-1}$  but only  $v = 30$  V  $s^{-1}$  if  $k_{AB}^- = 1.1 \times 10^3$   $s^{-1}$ . In fact, no peak for  $A^-$  was seen<sup>2g,15</sup> in either DMF or butyronitrile at 25 °C up to 100 V  $s^{-1}$ , which effectively rules out the smaller value of  $k_{AB}^-$ .

In addition, we may calculate a free energy of activation at 25 °C corresponding to each rate constant: 11.0 kcal  $mol^{-1}$  for  $k_{AB}^- = 5 \times 10^4$   $s^{-1}$  and 13.3 kcal  $mol^{-1}$  for  $k_{AB}^- = 1.1 \times 10^3$   $s^{-1}$ . Assuming the activation entropy to be small, one can use these values to estimate rate constants at any other temperature. Consider a series of voltammograms obtained at a constant sweep rate of 20 V  $s^{-1}$  but at lower and lower temperatures. When  $k_{AB}^-$  becomes about 800  $s^{-1}$ ,  $A^-$  will just begin to be detected. For  $k_{AB}^- = 1.1 \times 10^3$   $s^{-1}$  at 25 °C, this temperature of first detection is predicted to be 21 °C, whereas for  $k_{AB}^- = 5 \times 10^4$   $s^{-1}$ , it would be  $-28$  °C. In butyronitrile solvent, an  $A^-$  oxidation peak at 20 V  $s^{-1}$  was first detected<sup>2g</sup> at about  $-45$  °C, which is taken as additional evidence supporting the conclusion that  $k_{AB}^-$  at 25 °C is actually larger than the result obtained by pulse radiolysis.

The difference in rate constants observed for the two solvent systems may be caused by several factors. The reactions of anions with polar molecules can occur at rates as much as  $10^{10}$  greater in dipolar aprotic solvents than in protic solvents.<sup>16</sup> However, solvent effects on anionic isomerizations and other first-order reactions do not seem to have been studied. A reaction that bears some similarity to the  $A^- \rightarrow B^-$  reaction is the isomerization of *cis*-stilbene anion radical to *trans*-stilbene anion radical,<sup>17</sup> where it has been shown that ion-pair interactions play a crucial role. Generally, a solvent in which ion pairing is negligible gives much slower isomerization than a solvent where ion pairs are the dominant species. Such a factor could be active in the present case. For example, it is known that significant ion pairing occurs between tetraethylammonium ions and nitromesitylene anion radicals in DMF.<sup>18</sup>

In summary, the studies of the reduction of two bianthrone by homogeneous redox catalysis have confirmed the reduction mechanism that had been advanced on the basis of electrochemical and pulse radiolysis studies. The present system constitutes the first example of redox catalysis driven by a change in conformation as opposed to irreversible bond breaking. Interestingly, the two

(11) Richards, J. A.; Evans, D. H. *J. Electroanal. Chem. Interfacial Electrochem.* **1977**, *81*, 171-87.

(12) Nadjio, L.; Savčiant, J. M. *J. Electroanal. Chem. Interfacial Electrochem.* **1973**, *48*, 113-45.

(13) Evans, D. H. *J. Phys. Chem.* **1972**, *76*, 1160-5.

(14) Nicholson, R. S.; Shain, I. *Anal. Chem.* **1965**, *37*, 178-90.

(15) Evans, D. H.; Busch, R. W., unpublished results, 1982.

(16) (a) Parker, A. J. *Adv. Phys. Org. Chem.* **1967**, *5*, 173-235. (b) Buncel, E.; Wilson, H. *Ibid.* **1977**, *14*, 133-202.

(17) (a) Levin, G.; Ward, T. A.; Szwarc, M. *J. Am. Chem. Soc.* **1974**, *96*, 270-2. (b) Ward, T. A.; Levin, G.; Szwarc, M. *Ibid.* **1975**, *97*, 258-61. (c) Sorensen, S.; Levin, G.; Szwarc, M. *Ibid.* **1975**, *97*, 2341-5. (d) Chien, C. K.; Wang, H. C.; Szwarc, M.; Bard, A. J.; Itaya, K. *Ibid.* **1980**, *102*, 3100-4.

(18) Chauhan, B. G.; Fawcett, W. R.; Lasia, A. *J. Phys. Chem.* **1977**, *81*, 1476-81.

bianthrone fall in different kinetic zones, one in which the catalytic rate is governed by the forward electron-transfer reaction between quinone anion radicals and bianthrone and the other in which the catalytic rate is governed by the conformational change with electron transfer as a preequilibrium. The results provide additional evidence of the importance of conformational change in certain redox reactions and the efficacy of homogeneous redox catalysis in the study of such systems.

**Acknowledgment.** We thank Professor J. M. Savéant for tabulated theoretical data from ref 4e. This research was sup-

ported by the National Science Foundation (Grant CHE81-11421).

**Registry No.** 1, 434-85-5; 1 (radical anion), 70793-05-4; 2, 24541-19-3; 2 (radical anion), 79982-16-4; duroquinone, 527-17-3; 2-chloro-9,10-anthraquinone, 131-09-9; 2-methyl-1,4-naphthoquinone, 58-27-5; 2,6-dimethoxy-1,4-benzoquinone, 530-55-2; 2,5-di-*tert*-butyl-1,4-benzoquinone, 2460-77-7; duroquinone radical anion, 3572-98-3; 2-chloro-9,10-anthroquinone radical anion, 58272-39-2; 2-methyl-1,4-naphthoquinone radical anion, 34524-96-4; 2,6-dimethoxy-1,4-benzoquinone radical anion, 26547-64-8; 2,5-di-*tert*-butyl-1,4-benzoquinone radical anion, 3599-40-4.

## Intramolecular Electron Transfer and Dehalogenation of Nitroaromatic Anion Radicals<sup>1</sup>

J. P. Bays,<sup>2</sup> S. T. Blumer, S. Baral-Tosh, D. Behar,<sup>3</sup> and P. Neta\*<sup>4</sup>

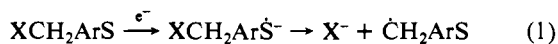
Contribution from the Radiation Laboratory and Departments of Chemistry, University of Notre Dame and St. Mary's College, Notre Dame, Indiana 46556.

Received March 15, 1982

**Abstract:** A series of nitroaromatic compounds, containing Cl, Br, or tosyl groups at various positions, were synthesized and studied by pulse radiolysis in aqueous alcohol solutions. One-electron reduction of the compounds produces the anion radicals which then undergo an intramolecular electron transfer and eliminate X<sup>-</sup> (Cl<sup>-</sup>, Br<sup>-</sup>, or TsO<sup>-</sup>). The rates of X<sup>-</sup> elimination vary over six orders of magnitude and are affected by the C-X bond dissociation energies, the size and nature of the group bridging the X with the  $\pi$  system, and the relative positions of these groups. Intramolecular electron transfer through space is also demonstrated.

### Introduction

One-electron reduction of aromatic compounds, which contain a halogen and an electron-affinic substituent, has been shown to produce initially an anion radical and subsequently to dehalogenate,<sup>5-14</sup> e.g.



The dehalogenation has been viewed as an intramolecular electron transfer reaction, where the added electron is initially at the  $\pi$  system of the substituent (S = NO<sub>2</sub>, CN, COR, etc.) and the aromatic ring and is later transferred to the C-X  $\sigma$  bond to form X<sup>-</sup> and a carbon-centered radical. The lack of significant overlap between the  $\pi$  system and the  $\sigma$  bond causes the delay in the electron transfer. The transition state must have considerable overlap of the  $\pi$  system with the partially broken  $\sigma$  bond. The rates of these processes have been found to vary over many orders of magnitude (from <1 s<sup>-1</sup> to >10<sup>7</sup> s<sup>-1</sup>) and are also dependent

on the nature of X and S and their relative positions on the molecule, i.e., the C-X bond strength, the electron affinity of S, and the charge density distribution in the anion radical.<sup>10-13</sup>

In the present study we have synthesized a number of halogen-substituted nitroaromatic compounds in order to examine in greater detail the effect of the C-X bond strength on the rate of dehalogenation and the importance of direct electron transfer from S<sup>-</sup> to a vicinal halogen through space rather than through the aromatic  $\pi$  system.

### Method

One-electron reduction and dehalogenation were monitored by kinetic spectrophotometric pulse radiolysis. The substrate was dissolved in *i*-PrOH or *t*-BuOH and then diluted with water. The solution was deoxygenated by bubbling with pure nitrogen or N<sub>2</sub>O and then irradiated with 10-ns 8-MeV electron pulses from an ARCO LP-7 linear accelerator. Each pulse produces 3-4  $\mu\text{M}$  total radical concentration. One-electron reduction is achieved by reaction of the substrate with either e<sub>aq</sub><sup>-</sup> or (CH<sub>3</sub>)<sub>2</sub>COH<sup>-</sup>. The details of these reduction processes under the various experimental conditions employed have been discussed previously.<sup>10-13</sup> The computer-controlled pulse radiolysis apparatus, which allows determination of transient spectra at various times after the pulse and kinetic measurements of the spectral changes, has also been described earlier.<sup>15</sup> This technique allows us to follow the formation and decay of the nitro anion radical, i.e., to directly determine absolute rate constants for the two steps in reaction 1.

### Results and Discussion

**$\alpha$ -Substitution on *p*-Nitrobenzyl Halides.** The rates of dehalogenation of the anion radicals of *p*-nitrobenzyl chloride and bromide were determined to be 4  $\times$  10<sup>3</sup> s<sup>-1</sup> and 1.7  $\times$  10<sup>5</sup> s<sup>-1</sup>, respectively.<sup>10</sup>  $\alpha$ -Substitution is expected to decrease the benzylic

(1) The research described herein was supported by the Office of Basic Energy Sciences of the Department of Energy. This is Document No. NDRL-2323 from the Notre Dame Radiation Laboratory.

(2) St. Mary's College.

(3) Soreq Nuclear Research Center, Yavne, Israel.

(4) Address correspondence to this author at the University of Notre Dame.

(5) Kornblum, N. *Angew. Chem., Int. Ed. Engl.* **1975**, *14*, 734, and references therein.

(6) Mohammad, M.; Hadju, J.; Kosower, E. M. *J. Am. Chem. Soc.* **1971**, *93*, 1792.

(7) Burrows, H. D.; Kosower, E. M. *J. Phys. Chem.* **1974**, *78*, 112.

(8) Lawless, J. G.; Bartak, D. E.; Hawley, M. D. *J. Am. Chem. Soc.* **1969**, *91*, 7121.

(9) Lawless, J. G.; Hawley, M. D. *J. Electroanal. Chem.* **1969**, *21*, 365.

(10) Neta, P.; Behar, D. *J. Am. Chem. Soc.* **1980**, *102*, 4798.

(11) Behar, D.; Neta, P. *J. Phys. Chem.* **1981**, *85*, 690.

(12) Neta, P.; Behar, D. *J. Am. Chem. Soc.* **1981**, *103*, 103.

(13) Behar, D.; Neta, P. *J. Am. Chem. Soc.* **1981**, *103*, 2280.

(14) Kigawa, H.; Takamuku, S.; Toki, S.; Kimura, N.; Takeda, S.; Tsu-mori, K.; Sakurai, H. *J. Am. Chem. Soc.* **1981**, *103*, 5176.

(15) Patterson, L. K.; Lilić, J. *Int. J. Radiat. Phys. Chem.* **1974**, *6*, 129.